

1  
2  
3 1 **Heterologous expression of a plant uracil transporter in yeast: improvement of**  
4  
5  
6 2 **plasma membrane targeting in mutants of the Rsp5p ubiquitin protein ligase**

7  
8 3 Froissard M<sup>&</sup>, Belgareh-Touzé N<sup>&</sup>, Buisson N<sup>&</sup>, Desimone M<sup>°</sup>, Frommer WB<sup>\$</sup> and  
9  
10  
11 4 Haguenaer-Tsapis R<sup>&\*</sup>.

12  
13  
14  
15 5 <sup>&</sup>Institut Jacques Monod-CNRS, Université Paris VI and Paris VII 2 place Jussieu  
16  
17 6 75251 Paris Cedex 05 France

18  
19 7 <sup>°</sup> Plant Physiology, ZMBP, Auf der Morgenstelle 1, D-72076 Tübingen, Germany.

20  
21  
22 8 <sup>\$</sup>Carnegie Institution of Washington, Plant Biology, Stanford, California 94305-4101,  
23  
24 9 USA.

25  
26  
27 10 **Running title:** Functional expression of a plant transporter in yeast

28  
29 11 \*Corresponding author:

30  
31 12 Tel: 33 1 44 27 63 86

32  
33 13 Fax: 33 1 44 27 59 94

34  
35 14 E mail: haguenaer@ijm.jussieu.fr

36  
37 15

38  
39  
40  
41 16 Keywords: transporters, yeast, heterologous expression, Rsp5p, ubiquitin protein  
42  
43 17 ligase

44  
45 18  
46  
47  
48  
49  
50  
51  
52  
53  
54  
55  
56  
57  
58  
59  
60

1  
2  
3  
4  
5  
6  
7  
8  
9  
10  
11  
12  
13  
14  
15  
16  
17  
18  
19  
20  
21  
22  
23  
24  
25  
26  
27  
28  
29  
30  
31  
32  
33  
34  
35  
36  
37  
38  
39  
40  
41  
42  
43  
44  
45  
46  
47  
48  
49  
50  
51  
52  
53  
54  
55  
56  
57  
58  
59  
60

18 **Abstract:**

19 Plasma membrane proteins involved in transport processes play a crucial role in cell  
20 physiology. On account of these properties, these molecules are ideal targets for  
21 development of new therapeutic and agronomic agents. However, these proteins are  
22 of low abundance, which limits their study. Although yeast seems ideal for expressing  
23 heterologous transporters, plasma membrane proteins are often retained in  
24 intracellular compartments. We tried to find yeast mutants potentially able to improve  
25 functional expression of a whole set of heterologous transporters. We focused on  
26 *Arabidopsis thaliana* ureide transporter 1 (AtUPS1), previously cloned by functional  
27 complementation in yeast. Tagged versions of AtUPS1 remain mostly trapped in the  
28 endoplasmic reticulum and were able to reach slowly the plasma membrane. In  
29 contrast, untagged AtUPS1 is rapidly delivered to plasma membrane, where it  
30 remains in stable form. Tagged and untagged versions of AtUPS1 were expressed in  
31 cells deficient in the ubiquitin ligase Rsp5p, involved in various stages of the  
32 intracellular trafficking of membrane-bound proteins. *rsp5* mutants displayed further  
33 plasma membrane stabilization of untagged AtUPS1, and improved steady state  
34 amounts of tagged versions of AtUPS1. *rsp5* cells are thus powerful tools to solve the  
35 many problems inherent in heterologous expression of membrane proteins in yeast,  
36 including ER retention.

1  
2  
3 38 **Introduction:**  
4  
5  
6 39  
7

8 40 Systematic sequencing of the genomes of complex organisms (e.g., the plant  
9  
10 41 *Arabidopsis thaliana*, certain parasites, and man) has revealed a great number of  
11  
12 42 genes that are likely to code for membrane transporters [1]. Many of these proteins  
13  
14 43 are assigned to this functional category on the sole basis of sequence similarity to  
15  
16 44 known transport proteins. Their biochemical properties are thus unknown and  
17  
18 45 information regarding substrate specificity is often lacking. To possess such  
19  
20 46 knowledge would be important both scientifically and industrially, because transport  
21  
22 47 proteins (channels, pumps, and carriers) play a crucial role in cell physiology. This is  
23  
24 48 illustrated by the numerous genetic diseases that are caused by defective transport  
25  
26 49 systems. Furthermore, cell surface membrane transporters may be ideal targets for  
27  
28 50 the development of new therapeutic or agronomic agents. Biological systems are  
29  
30 51 thus required for the functional expression of each transport protein and for the study  
31  
32 52 of its biochemical properties by means of quick, simple tests. The yeast  
33  
34 53 *Saccharomyces cerevisiae* expression system best meets these requirements. It is  
35  
36 54 easy to use and inexpensive, its "transportome" has been extensively analyzed *in*  
37  
38 55 *silico* [2,3] and the function of over 150 yeast transport proteins has been identified  
39  
40 56 [4]. Moreover, the construction of a complete collection of strains deleted for each of  
41  
42 57 the 6200 yeast genes [5] led to an impressive number of *S. cerevisiae* mutants  
43  
44 58 deficient in the transport of compounds as diverse as inorganic ions, metabolites, and  
45  
46 59 drugs. The phenotypes of these mutants are easily identified after growth on solid  
47  
48 60 media and have been used extensively in complementation tests, notably to clone  
49  
50 61 and characterize heterologous transporters.  
51  
52  
53  
54  
55  
56  
57  
58  
59  
60

1  
2  
3  
4 62 Hundreds of plant transporters have been successfully cloned by  
5  
6 63 complementation in yeast [6-9]. The yeast system has also been used in biochemical  
7  
8 64 approaches, for example, to analyze the functional properties of plant H<sup>+</sup>-ATPases  
9  
10 65 [10]. Nevertheless, although yeast seems ideal for expressing plasma membrane  
11  
12 66 proteins including transporters and receptors, investigators often found some of  
13  
14 67 these proteins to be inactive in yeast, sometimes because the protein did not fold  
15  
16 68 properly and/or was not delivered to the plasma membrane but accumulated in a  
17  
18 69 secretory compartment (endoplasmic reticulum (ER), Golgi apparatus, secretory  
19  
20 70 vesicles), sometimes even leading to formation of karmellae [11]. On the other hand,  
21  
22 71 some heterologous proteins correctly delivered to the plasma membrane have been  
23  
24 72 described to undergo rapid endocytosis and turnover, resulting in low plasma  
25  
26 73 membrane levels [12].

27  
28  
29  
30  
31  
32 74 A few attempts to improve functional expression in yeast of heterologous  
33  
34 75 plasma membrane transporters have been reported, but they often focused on only  
35  
36 76 one given transporter [13,14]. Attempts to identify yeast mutants that would  
37  
38 77 potentially improve the functional expression of a whole set of plasma membrane  
39  
40 78 proteins and more specifically transporters, are still lacking. Finding such mutants for  
41  
42 79 improvement of the functional expression of several plant and mammalian  
43  
44 80 transporters was the objective of an European network, EFFEXPORT ("Engineering  
45  
46 81 yeast for efficient expression of heterologous membrane transporters"). We report  
47  
48 82 here data we obtained within EFFEXPORT in the case of the *Arabidopsis Thaliana*  
49  
50 83 ureide transporter (AtUPS1), already known to be functionally expressed in *S.*  
51  
52 84 *cerevisiae* [15]. AtUPS1, was identified by functional complementation of a yeast *dal4*  
53  
54 85 *dal5* mutant [15] defective in uptake of allantoin. AtUPS1 belongs to a superfamily of  
55  
56 86 plant transporters with five members in Arabidopsis. Analysis of hydrophobicity

1  
2  
3 87 predicts 10 putative transmembrane domains, with N- and C-termini predicted to  
4  
5 88 protrude into the extracellular space. UPS proteins display a conserved central  
6  
7  
8 89 domain between predicted transmembrane helices 5 and 6, which contains a  
9  
10 90 consensus sequence for a P loop, also designated as a « Walker A » motif for ATP  
11  
12 91 binding [15]. Expression in yeast and *Xenopus* oocytes allowed to demonstrate that  
13  
14 92 *AtUPS1* mediates uptake of allantoin and related metabolites including uracil [15,16].  
15  
16 93 The fate of *AtUPS1* can thus be compared to that of the endogenous uracil  
17  
18 94 permease (*Fur4p*), a well-known yeast transporter, the trafficking of which has been  
19  
20 95 studied extensively (reviewed in [17]). *Fur4p*, which belongs to a family of five  
21  
22 96 homologous proteins in *S. cerevisiae* [2], also consists of ten transmembrane spans,  
23  
24 97 with cytoplasmic oriented N- and C- termini [18]. Like most yeast plasma membrane  
25  
26 98 proteins, it displays plasma membrane ubiquitylation, catalyzed by the *Rsp5p*  
27  
28 99 ubiquitin protein ligase, a modification triggering its internalization and subsequent  
29  
30 100 vacuolar degradation [19]. The same ubiquitin ligase, the sole member of the family  
31  
32 101 of *Nedd4* ubiquitin ligases in yeast [20], was also demonstrated to be required for  
33  
34 102 direct Golgi-to-vacuole trafficking of a number of plasma membrane transporters,  
35  
36 103 including *Fur4p* [17,21], *i.e.* proteins routed to a direct degradation pathway  
37  
38 104 bypassing the plasma membrane under certain nutrient/substrate conditions. *Rsp5p*  
39  
40 105 was also described to be required for Golgi-to-vacuole traffic of misfolded plasma  
41  
42 106 membrane proteins misrouted to the vacuole [22]. In latter two cases, these proteins  
43  
44 107 were retargeted to plasma membrane in *rsp5* mutants. *rsp5* mutants thus display  
45  
46 108 increased steady state amounts of many plasma membrane transporters (reviewed  
47  
48 109 in [17]), and were good candidates for potential improvement of functional expression  
49  
50 110 of heterologous transporters. However, in addition to its role in trafficking of  
51  
52 111 membrane proteins [17], *Rsp5p* has many other functions, including essential  
53  
54  
55  
56  
57  
58  
59  
60

1  
2  
3 112 functions [23,24]. Hence, only defined *rsp5* mutants may be used for optimization of  
4  
5 113 functional expression of heterologous proteins. Two viable *rsp5* mutants that were  
6  
7  
8 114 described to be affected for several of the trafficking functions of Rsp5p appeared  
9  
10 115 interesting: *npi1* mutant, with altered *RSP5* promoter, leading to a 10-fold reduction in  
11  
12 116 the steady state amount of this protein [25], and *rsp5ΔC2*, lacking Rsp5p C2 domain  
13  
14 117 involved in localization of the enzyme at plasma membrane and endosomes [26].  
15  
16  
17

18  
19 118 We report here an analysis of the fate of AtUPS1, as compared to that of  
20  
21 119 Fur4p, in wild type and *rsp5* mutant cells, and show that *npi1* and *rsp5ΔC2* cells  
22  
23 120 improved functional expression of the plant transporter.  
24  
25  
26

27 121

## 28 29 122 **Results**

30 123

### 31 124 **AtUPS1 mediates high affinity uracil transport in yeast**

32  
33  
34  
35  
36 125 As outlined above, when expressed in yeast, AtUPS1 transports [<sup>14</sup>C] labelled  
37  
38 126 allantoin with high affinity and potentially other heterocyclic compounds as suggested  
39  
40 127 by competition studies [15]. Moreover, AtUPS1 mediates uracil uptake when  
41  
42 128 expressed in *Xenopus* oocytes [16]. In order to monitor the intracellular fate of  
43  
44 129 AtUPS1 in yeast, *UPS1* was cloned in a multicopy plasmid under the control of the  
45  
46 130 galactose-inducible GAL promoter. We defined the characteristics of uracil uptake  
47  
48 131 mediated by GAL-*UPS1*, as compared to uracil uptake mediated by the endogenous  
49  
50 132 Fur4p cloned under the control of the same promoter. *fur4Δ* cells grown on galactose  
51  
52 133 expressing either GAL-*UPS1* or GAL-*FUR4* displayed high sensitivity to 5-fluorouracil  
53  
54 134 (5FU), a toxic analog of uracil: cells expressing the transporters were unable to grow  
55  
56 135 on plates containing 1μM 5FU, whereas cells transformed with a control plasmid  
57  
58  
59  
60

1  
2  
3 136 grew normally (Fig 1A). To determine the uracil transport properties of AtUPS1  
4  
5  
6 137 quantitatively, radiotracer uptake studies were performed using [<sup>14</sup>C] uracil. [<sup>14</sup>C]  
7  
8 138 uracil uptake mediated by GAL-*UPS1* expressed in *fur4Δ* cells growing exponentially  
9  
10  
11 139 and fully induced on galactose was linear for at least 3 min, concentration-  
12  
13 140 dependent, and displayed saturation kinetics with an apparent *K<sub>m</sub>* of 6 μM, close to  
14  
15  
16 141 that observed in parallel for cells expressing GAL-*FUR4* (7.5 μM). *fur4Δ* cells  
17  
18 142 expressing GAL-*UPS1* grown overnight in galactose containing media displayed an  
19  
20 143 activity 50% of cells expressing GAL-*FUR4*, *i.e.*, more than 30-fold that of  
21  
22 144 chromosomal encoded *FUR4* (Fig. 1B), thus providing a sensitive assay to follow  
23  
24 145 AtUPS1 intracellular fate.  
25  
26  
27  
28 146

### 30 147 **Insight into AtUPS1 intracellular trafficking in yeast**

32 148 Inducibility of AtUPS1 synthesis after galactose induction provides a useful  
33  
34 149 tool for monitoring plasma membrane delivery, as previously demonstrated for the  
35  
36 150 yeast Fur4p [27]. We measured uracil uptake activity after galactose induction of  
37  
38 151 GAL-*UPS1* and GAL-*FUR4* in *fur4Δ* cells in parallel (Fig. 2A). In both cases, activity,  
39  
40 152 as a measure of plasma membrane targeting, was detectable after 30 min induction.  
41  
42 153 The increase in uracil uptake activity was linear for one hour with a similar slope for  
43  
44 154 cells expressing the yeast and the plant transporters. Hence the heterologous  
45  
46 155 AtUPS1 appears to be recognized efficiently by the yeast secretory machinery. We  
47  
48 156 then compared the fate of AtUPS1 and Fur4p along the endocytic pathway using an  
49  
50 157 experimental condition known to trigger rapid Fur4p internalization and subsequent  
51  
52 158 vacuolar degradation, *i. e.* the inhibition of protein synthesis by addition of  
53  
54 159 cycloheximide [28] (Fig. 2B). Cycloheximide was added to exponentially growing  
55  
56 160 *fur4Δ* cells induced overnight in galactose for expression of either AtUPS1 or Fur4p.  
57  
58  
59  
60

1  
2  
3 161 Uracil uptake activity of cells expressing Fur4p decreased rapidly ( $t_{1/2} = 45$  min),  
4  
5  
6 162 whereas uracil uptake activity of cells expressing AtUPS1 did not display a decrease  
7  
8 163 for four hours. Hence, once delivered to the plasma membrane, the plant AtUPS1  
9  
10 164 was remarkably stable, and did not undergo obvious endocytosis after inhibition of  
11  
12 165 protein synthesis.  
13  
14

15 166

### 17 167 **C-terminally tagged versions of AtUPS1 are retained in the ER**

18  
19  
20 168 The monitoring of uracil uptake activity can afford insight into the intracellular  
21  
22 169 fate of AtUPS1, since it provides information about the plasma membrane located  
23  
24 170 transporter. This information, however, remains limited, and does not indicate the  
25  
26 171 fraction of plasma membrane-delivered protein versus potential intracellular pools. In  
27  
28 172 the absence of available antibodies, we decided to monitor the fate of tagged  
29  
30 173 versions of AtUPS1. C-terminally tagged versions of AtUPS1 were constructed, first  
31  
32 174 with a GFP-tag, a powerful tool for monitoring the intracellular fate in yeast of plasma  
33  
34 175 membrane proteins of heterologous [14] or endogenous origin, including that of  
35  
36 176 Fur4p [29-31]. *fur4Δ* cells transformed with a multicopy plasmid carrying *GAL-UPS1-*  
37  
38 177 *GFP* displayed high 5FU sensitivity after growth on galactose (Fig. 3A). Strikingly,  
39  
40 178 *fur4Δ* cells transformed with multicopy plasmid carrying *GAL-UPS1* tagged with the  
41  
42 179 smaller HA epitope displayed intermediate 5FU sensitivity after growth on galactose,  
43  
44 180 indicating that a smaller tag did not improve AtUPS1 functionality. According to these  
45  
46 181 plate assays, C-terminally tagged AtUPS1 thus appeared functional, notably GFP-  
47  
48 182 tagged AtUPS1. However, *fur4Δ* cells transformed by the multicopy plasmid carrying  
49  
50 183 *GAL-UPS1-GFP* and fully induced displayed only a very low level of uracil uptake  
51  
52 184 activity (0.04 nMol/min/A<sub>600</sub>), an activity 50 fold lower than that observed in the case  
53  
54 185 of induced cells transformed by a plasmid carrying untagged AtUPS1 (not shown).  
55  
56  
57  
58  
59  
60

1  
2  
3 186 The use of a smaller tag (HA) or another promoter (CYC1) did not improve uracil  
4  
5 187 uptake activity.  
6  
7

8 188 The GFP -or HA- tags may inhibit transport activity or impair plasma  
9  
10 189 membrane delivery of tagged transporter due to folding problems. We checked GFP  
11  
12 190 fluorescence in time course experiments using the multicopy plasmid carrying the  
13  
14 191 *GAL-UPS1-GFP* (Fig. 3B), or the multicopy plasmid *GAL-Fur4-GFP* as a control.  
15  
16 192 Galactose induction of *Fur4-GFP* led, after 30 min, to observation of small internal  
17  
18 193 compartments, likely Golgi/secretory vesicles. 30 min later, plasma membrane  
19  
20 194 staining was clearly evidenced, often in a polarized fashion, with intense staining of  
21  
22 195 small buds (Fig. 3B). The distribution of *AtUPS1-GFP* was strikingly different. After  
23  
24 196 30 min of galactose induction of *AtUPS1-GFP* expression, a perinuclear staining was  
25  
26 197 clearly observable. 30 min later, or after overnight induction, the perinuclear staining  
27  
28 198 was still present and a discontinuous staining at/or underneath the plasma  
29  
30 199 membrane has appeared. This pattern is typical of the yeast ER. Intense staining of  
31  
32 200 lines or spots, as if intracellular membranes had formed aggregates were also  
33  
34 201 visualized (Fig. 3B). Indeed, electron microscopy of the ultrastructural morphology of  
35  
36 202 cells fully induced for expression of *AtUPS1-GFP* revealed proliferation, hanks of ER  
37  
38 203 membranes (Fig. 3D), as often described in the case of cells overexpressing ER-  
39  
40 204 retained proteins [11]. This altered morphology did not resulted from the  
41  
42 205 overexpression of a membrane protein as such: overnight overexpression of  
43  
44 206 endogenous *FUR4* from the same multicopy, GAL-inducible plasmid, did not lead to  
45  
46 207 altered morphology (not shown).  
47  
48  
49  
50  
51  
52  
53

54  
55 208 ER-retention of GFP-tagged *AtUPS1* apparently did not result from the mere  
56  
57 209 overexpression of this protein. Perinuclear/ER staining was also evidenced upon  
58  
59 210 expression of *AtUPS1-GFP* from a centromeric plasmid under the control of the mild  
60

1  
2  
3 211 strength *CYC1* promoter, leading to a steady state protein level about 4-fold lower  
4  
5 212 than that observed after two hours galactose induction of GAL-*UPS1-GFP* (Fig. 3B  
6  
7 213 and C). Furthermore, when analyzed by sucrose gradient fractionation, AtUPS1-GFP  
8  
9 214 expressed from the CEN *CYC1*-plasmid or from the 2  $\mu$  GAL-inducible plasmid  
10  
11 215 displayed exactly the same pattern with major pool in internal fractions (data not  
12  
13 216 shown).

14  
15  
16  
17 217 Hence, the GFP tag at the C-terminus of AtUPS1 obviously triggers ER  
18  
19 218 retention of the transporter. The low uracil uptake activity of cells expressing this  
20  
21 219 transporter can only be observed after long expression periods (3-4 hours, cf Fig.  
22  
23 220 6B), and likely corresponds to the low fraction of protein finally reaching the plasma  
24  
25 221 membrane. With such folding problems, overexpression is a way to increase steady  
26  
27 222 state plasma membrane expression: both 5FU sensitivity and uracil uptake activity  
28  
29 223 were improved in the case of AtUPS1-GFP expression from a multicopy plasmid and  
30  
31 224 strong GAL promoter compared to expression from a centromeric plasmid under the  
32  
33 225 control of a lower strength promoter.  
34  
35  
36  
37  
38  
39  
40

#### 41 227 **Intracellular fate of AtUPS1 carrying an internal myc tag in yeast: slow ER exit** 42 43 228 **but final plasma membrane delivery**

44  
45  
46 229 We checked whether insertion of a small myc-tag inside the central loop  
47  
48 230 containing the Walker A motif would be a better way to study AtUPS1 intracellular  
49  
50 231 trafficking. Cells expressing internally myc tagged AtUPS1 from a multicopy  
51  
52 232 galactose inducible plasmid displayed high sensitivity to 5FU (Fig. 4A). Cells  
53  
54 233 transformed with the multicopy GAL-*UPS1<sup>myc</sup>* plasmid grown overnight in galactose  
55  
56 234 displayed a relatively high level of uracil uptake activity: 1 nMol/min/A<sub>600</sub>, *i. e.* 70%  
57  
58 235 that observed in the case of untagged AtUPS1 (Fig. 4B), suggesting that the myc tag  
59  
60

1  
2  
3 236 at this position had only a small impact on AtUPS1 function. However, this tag had a  
4  
5 237 clear influence on AtUPS1 intracellular trafficking. Induction experiments showed that  
6  
7  
8 238 uracil uptake activity appeared slowly: 4-6 hours were necessary before we were  
9  
10 239 able to measure any detectable uptake activity (Fig. 4C). Aliquots withdrawn at  
11  
12 240 several time points after galactose induction were analyzed by protein gel blots using  
13  
14  
15 241 a specific anti-myc antibody. AtUPS1<sup>myc</sup> appeared on gels as a band of apparent  
16  
17  
18 242 molecular mass of about 36 kDa, *i. e.* slightly below the expected molecular mass  
19  
20 243 deduced from predicted protein sequence (44 kDa) (Fig. 4E), as often observed for  
21  
22 244 very hydrophobic proteins. A comparable pattern was observed after overnight  
23  
24  
25 245 galactose induction of AtUPS1<sup>myc</sup> expressed from either a centromeric or a multicopy  
26  
27  
28 246 plasmid (data not shown).

29  
30 247 In order to check the intracellular location of AtUPS1<sup>myc</sup> derived species, cells  
31  
32 248 transformed with GAL-UPS1<sup>myc</sup> were induced by addition of galactose, aliquots  
33  
34  
35 249 withdrawn periodically were fixed and analyzed by immunofluorescence using a  
36  
37 250 monoclonal anti-myc antibody. One hour induction was sufficient to observe a  
38  
39 251 specific signal, mostly perinuclear, supported by simultaneous DAPI staining (Fig.  
40  
41 252 5A). To obtain better resolution of the cell surface staining (potentially corresponding  
42  
43 253 to either ER or plasma membrane), cells were examined by confocal microscopy.  
44  
45  
46 254 The lower background in optical slices made it possible to show that all cells  
47  
48  
49 255 displayed perinuclear staining, together with discontinuous regions of cell surface  
50  
51 256 staining (Fig. 5B). Because cell surface was not homogeneously stained, we can  
52  
53 257 conclude that the main signal corresponds to ER staining and that a plasma  
54  
55 258 membrane localisation cannot be detected by this approach. The low rate of uracil  
56  
57 259 uptake activity thus likely resulted from low ER exit rates (Fig. 4C) The finding that  
58  
59  
60 260 the activity of fully induced cells is in a similar range as that of cells expressing

1  
2  
3 261 untagged AtUPS1, which was rapidly targeted to plasma membrane, may suggest  
4  
5 262 that after slow rates of ER exit, AtUPS1<sup>myc</sup> finally reached the plasma membrane.  
6  
7 263 Further indication that AtUPS1<sup>myc</sup> stored in internal compartments could finally reach  
8  
9 264 plasma membrane was provided by the observation of some increase in uracil  
10  
11 265 uptake activity after stopping transporter synthesis by the addition of CHX (Fig. 4D).  
12  
13 266 Once targeted at the plasma membrane, AtUPS1<sup>myc</sup> was rather stable, as judged  
14  
15 267 from the extreme stability of uracil uptake activity for over 3 hours after this transient  
16  
17 268 uracil uptake activity increase following CHX addition. However, some low rate  
18  
19 269 endocytosis likely occurred as compared to the incredibly stable untagged AtUPS1  
20  
21 270 (Fig. 4D).  
22  
23  
24  
25  
26  
27  
28  
29  
30  
31

### 32 273 **Mutations in the Rsp5 ubiquitin protein ligase improve functional expression of** 33 34 274 **tagged and untagged AtUPS1 in yeast**

35  
36 275 Despite the difficulties encountered in tagging AtUPS1 at different positions,  
37  
38 276 the high sensitivity of the two functional tests, 5FU sensitivity and uracil uptake  
39  
40 277 measurements, provided suitable tools to check whether yeast mutants could  
41  
42 278 improve the steady state levels of functional tagged or untagged AtUPS1 versions.  
43  
44 279 We used two viable *rsp5* mutants, *npi1* and *rsp5ΔC2*, that display delayed  
45  
46 280 endocytosis of several cargoes, including Fur4p. Accordingly, they displayed  
47  
48 281 increased 5FU sensitivity as a result of the plasma membrane stabilization of  
49  
50 282 endogenous chromosomal or plasmid encoded Fur4p (not shown). We checked the  
51  
52 283 fate of tagged and untagged versions of AtUPS1 in *npi1* and *rsp5ΔC2* mutant cells.  
53  
54  
55  
56  
57

58 284 For this purpose, *FUR4* was deleted in wild type, *npi1* and *rsp5ΔC2* cells, and  
59  
60 285 the resulting strains were transformed with multicopy plasmids carrying either *UPS1*

1  
2  
3 286 under the control of the constitutive PGK promoter (plasmid pFL61-*UPS1*), or  
4  
5 287 galactose inducible *UPS1*, *UPS1-GFP* and *UPS1<sup>myc</sup>*. Transformed cells grown in  
6  
7  
8 288 glucose, or galactose containing media in the case of plasmids with a GAL promoter  
9  
10 289 displayed identical growth in the absence of 5FU (Fig. 6A), indicating that neither the  
11  
12 290 mutations, nor the expression of the plant transporters impaired growth. 5FU  
13  
14 291 sensitivity of transformants was strikingly enhanced in both *rsp5ΔC2* and *npi1* cells  
15  
16 292 expressing the tagged and untagged plant transporter when compared to wild type  
17  
18 293 cells, with slightly stronger effect promoted in all cases by the *npi1* mutation  
19  
20 294 (compare the size of isolated colonies) (Fig. 6A). This suggests higher amounts of  
21  
22 295 plasma membrane tagged or untagged transporters in the mutants. In the case of the  
23  
24 296 untagged transporters, the enhancement in 5FU sensitivity was evidenced after  
25  
26 297 synthesis from PGK or *GAL10* promoter at different 5FU concentrations (Fig. 6A),  
27  
28 298 indicating that *rsp5* mutations interfered with trafficking, rather than with galactose-  
29  
30 299 driven expression. For untagged AtUPS1 which is rapidly delivered to the plasma  
31  
32 300 membrane and very stable in wild type cells, the increase in functional transporter  
33  
34 301 activity observed in *rsp5*  $\alpha$ mutants may result from inhibition of some direct Golgi to  
35  
36 302 vacuole targeting, or from protection against a possible low basal endocytosis, for  
37  
38 303 instance when cells reached stationary phase, a likely situation for cells grown  
39  
40 304 several days on plates.  
41  
42  
43  
44  
45  
46  
47

48 305 In the case of the myc-tagged version of AtUPS1, we monitored the fate of the  
49  
50 306 transporter after galactose induction by western blots (Fig 6C), and uracil uptake  
51  
52 307 measurements (Fig. 6B). In agreement with fluorescent data, AtUPS1<sup>myc</sup> protein was  
53  
54 308 already detectable in wild type cells at early time points after induction (30-60 min)  
55  
56 309 but uracil uptake was readily measurable only at far later time points (4 hours). In  
57  
58 310 *npi1* cells, AtUPS1<sup>myc</sup> was detectable in higher amounts at all time points and uracil  
59  
60

1  
2  
3 311 uptake activity appeared at least one hour earlier compared to wild type cells (Fig.  
4  
5 312 6B). *rsp5ΔC2* mutation also resulted in more rapid appearance of uracil uptake  
6  
7  
8 313 activity. Strikingly, even if the activity was lower for cells expressing AtUPS1-GFP  
9  
10 314 compared to AtUPS1<sup>myc</sup>, the rate of appearance of uptake was very similar. For both  
11  
12 315 types of tagged transporters uracil uptake activity was thus 2-3 fold higher in mutant  
13  
14 316 cells than in wild type cells after 4 hour induction. Since the major pool of both  
15  
16 317 AtUPS1-GFP and AtUPS1<sup>myc</sup> seemed to be in the ER, both *npi1* and *rsp5ΔC2*  
17  
18 318 mutations apparently lead to accelerated ER exit.  
19  
20  
21  
22  
23  
24

319

## 320 Discussion:

25  
26  
27 321 The use of a regulable promoter and the high sensitivity of uracil uptake  
28  
29 322 measurements enabled us to obtain crucial information about the fate of untagged  
30  
31 323 AtUPS1 uracil transporter in yeast. AtUPS1 is rapidly delivered to the plasma  
32  
33 324 membrane, with kinetics indistinguishable from those of endogenous yeast  
34  
35 325 transporter. Hence, the yeast secretory pathway efficiently handles the heterologous  
36  
37 326 plant transporter. It is possible that such property was the reason for the successful  
38  
39 327 cloning by functional expression of so many plant transporters when using yeast as a  
40  
41 328 host system [6,7]. Plasma membrane delivered AtUPS1 exhibited striking stability,  
42  
43 329 notably when compared to the endogenous yeast uracil permease especially  
44  
45 330 susceptible to stress-induced endocytosis [28]. This was true for both untagged  
46  
47 331 transporter and for internally tagged AtUPS1<sup>myc</sup> (not shown). This differential stability  
48  
49 332 between yeast and plant uracil transporters may possibly reflect fundamental  
50  
51 333 differences in their endocytic processes. Endocytosis in yeast is dependent on prior  
52  
53 334 ubiquitylation of plasma membrane cargoes by the Rsp5p ubiquitin protein ligase  
54  
55 335 [17]. A subset of mammalian proteins undergo ubiquitin-dependent endocytosis,  
56  
57  
58  
59  
60

1  
2  
3 336 sometimes involving ubiquitin-protein ligases of the Nedd4/Rsp5 family [32]. In  
4  
5  
6 337 contrast, although plants display numerous ubiquitin protein ligases, they do not  
7  
8 338 seem to have Rsp5p orthologs [33]. The extreme stability of AtUPS1 in yeast could  
9  
10 339 result from the absence or low accessibility of ubiquitylation sites that Rsp5p can  
11  
12 340 recognize, at least under the experimental conditions we tested. One possible reason  
13  
14  
15 341 could be the luminal orientation of both AtUPS1 N- and C-termini.  
16

17 342 In addition to obtaining information on intracellular trafficking of the plant  
18  
19 343 AtUPS1 in yeast based on uptake measurements, we tried to gain new insights into  
20  
21 344 the biochemical properties of this transporter. Unfortunately, tagging the transporter,  
22  
23 345 either at the N-terminus (not shown) and C-terminus or inside its central loop, lead to  
24  
25 346 folding problems, often resulting in ER retention of most of the protein, preventing us  
26  
27 347 from using these tagged versions to obtain a judicious biochemical characterization  
28  
29 348 of this transporter. A marked difference, however, was observed between internal  
30  
31 349 tagging, and tagging at the N- and C-termini, which was far more deleterious.  
32  
33 350 Internally tagged transporter displayed delayed ER exit, but finally reached the  
34  
35 351 plasma membrane in a fully functional state, and fully induced cells expressing this  
36  
37 352 version of the transporter displayed activity closely resembling that of cells  
38  
39 353 expressing untagged transporter. In contrast, cells expressing C-terminally tagged  
40  
41 354 transporter displayed 40-fold less uracil uptake activity compared to cells expressing  
42  
43 355 untagged transporters, probably because of a very low percentage of the protein  
44  
45 356 exiting the ER. In latter case, some improvement could be achieved by increased  
46  
47 357 levels of expression (stronger promoter, multicopy versus centromeric plasmid). The  
48  
49 358 deleterious effect of C-terminal tags could result from the unusual structure of the  
50  
51 359 transporter. Hydrophobicity plot analysis of proteins of the UPS family suggested an  
52  
53 360 external orientation of both termini [15] a situation somewhat rare for transporters.  
54  
55  
56  
57  
58  
59  
60

1  
2  
3 361 Most yeast transporters, for instance, display cytoplasmic oriented termini, as  
4  
5 362 predicted from hydrophobicity plot analysis or from experimental data [2]. Many of  
6  
7 363 these transporters were studied after tagging, most often at their C-terminus, a  
8  
9 364 modification that did not induce any major trafficking problems. The observation that  
10  
11 365 N- and C-terminal tags impaired AtUPS1 folding is compatible with an external  
12  
13 366 orientation, but experimental data are required to prove this. One obvious lesson  
14  
15 367 from these observations is that tagging at the positions and with the tags used in the  
16  
17 368 present study may probably influence the fate of UPS proteins in plant cells in a  
18  
19 369 similar way as in yeast cells. Indeed, previous studies attempting to study the  
20  
21 370 subcellular location of N- or C-terminal fusions of UPS proteins with GFP by transient  
22  
23 371 expression in Arabidopsis protoplasts showed that these fusion proteins did not  
24  
25 372 reach the plasma membrane (Schmidt, A., Baumann, N. and Desimone, M.,  
26  
27 373 unpublished data). This suggests that yeast may also represent a useful  
28  
29 374 experimental system to decipher where tags can be introduced in heterologous  
30  
31 375 transporters.  
32  
33  
34  
35  
36  
37

38 376 The distinctive behaviour of the various versions of AtUPS1, one correctly  
39  
40 377 targeted to the plasma membrane, and two retained in the ER to various extents,  
41  
42 378 provided the opportunity to check how to improve the steady state plasma membrane  
43  
44 379 amount of heterologous transporters with distinct intracellular fates. We checked  
45  
46 380 specifically the influence of mutations in Rsp5p. This ubiquitin protein ligase is  
47  
48 381 involved in various stages of intracellular trafficking of membrane-bound proteins,  
49  
50 382 including ER-associated degradation, plasma membrane internalization, Golgi to  
51  
52 383 vacuolar trafficking, and sorting to multivesicular bodies [17]. Limiting or preventing  
53  
54 384 latter three trafficking steps results in elevated steady state levels of yeast  
55  
56 385 transporters. Two specific viable mutants were used, *npi1*, with decreased amounts  
57  
58  
59  
60

1  
2  
3 386 of Rsp5p [25] and *rsp5ΔC2*, lacking the C2 domain of Rsp5p [34], dispensable for  
4  
5  
6 387 viability, but critical for Rsp5p trafficking functions [26,34-38]. Strikingly, both mutants  
7  
8 388 improved steady state amounts of functional, plasma membrane targeted, tagged  
9  
10 389 and untagged versions of AtUPS1, as judged from increased 5FU sensitivity. In the  
11  
12 390 case of untagged transporter, increased 5FU sensitivity was observed after  
13  
14  
15 391 expression of the transporter under the control of the constitutive PGK promoter, or  
16  
17 392 the inducible *GAL10* promoter, indicating that the mutations interfered as expected  
18  
19 393 with trafficking rather than with expression.

20  
21  
22 394 In the case of the untagged version of AtUPS1, it was difficult to further  
23  
24 395 explore the mechanism of this improvement. Plasma membrane AtUPS1 was so  
25  
26 396 stable in wild type cells submitted to CHX treatment that further stabilisation in *rsp5*  
27  
28 397 cells could not be detected in this type of experiment. The improvement in plasma  
29  
30 398 membrane steady state amounts of AtUPS1 in *npi1* and *rsp5ΔC2* cells might possibly  
31  
32 399 arise from a low basal endocytosis of AtUPS1, undetectable in CHX chase  
33  
34 400 experiments, but possibly occurring once cells reach stationary phase, as is the case  
35  
36 401 for cells grown on plates. Alternatively, the increase in plasma membrane AtUPS1 in  
37  
38 402 these *rsp5* mutants could result from a decreased direct Golgi to vacuole targeting of  
39  
40 403 a fraction of the transporter.

41  
42 404 Mutations in *RSP5*, either *npi1* or *rsp5ΔC2*, had a similar impact on the  
43  
44 405 intracellular fate of tagged versions of AtUPS1 at both the C-terminus or in the  
45  
46 406 intracellular loop. These two variants of AtUPS1 were mainly located in the ER, with  
47  
48 407 possibly exit in only very limited amounts (AtUPS1-GFP), or more important final  
49  
50 408 amounts (AtUPS1<sup>myc</sup>) thus leading to uracil uptake activity similar to that displayed by  
51  
52 409 cells expressing untagged transporters. In both cases, the rate of plasma membrane  
53  
54 410 delivery of uracil uptake activity was greatly delayed, with activity measurable after 3-

1  
2  
3 411 4 hours induction instead of 30 min for AtUPS1 –i. e. long after detection of the  
4  
5 412 protein on Western blots- and the two *rsp5* mutations reduced this delay. At first  
6  
7 413 glance, this effect can be attributed to an effect of Rsp5p on ER exit. Among its many  
8  
9 414 functions, Rsp5p was described to be involved in ubiquitylation followed by  
10  
11 415 proteasome degradation of several misfolded soluble and membrane-bound proteins  
12  
13 416 retained in the ER, notably under conditions of saturation of other ER-associated  
14  
15 417 degradative (ERAD) pathways [39]. Tagged forms of AtUPS1 might be partly  
16  
17 418 susceptible to such an Rsp5p-dependent ER-associated degradation, and inhibition  
18  
19 419 of this degradation in *npi1* and *rsp5ΔC2* mutants would result in more rapid ER exit of  
20  
21 420 transporters escaping this degradation to some extent. It is also possible that a small  
22  
23 421 number of misfolded tagged transporters undergo ER to Golgi trafficking, followed by  
24  
25 422 Golgi to vacuole sorting. Rsp5p was also shown to be involved in Golgi to vacuole  
26  
27 423 trafficking of some misfolded mutant plasma membrane proteins [22] or of yeast  
28  
29 424 transporters displaying direct vacuolar targeting under specific nutrient conditions  
30  
31 425 [17]. In both cases in *rsp5* mutants, these proteins are directed to plasma membrane  
32  
33 426 [22,40]. A small fraction of tagged AtUPS1 could undergo such direct vacuolar  
34  
35 427 trafficking, a process inhibited in *rsp5* mutants. In support of a partial direct Golgi to  
36  
37 428 vacuole trafficking of AtUPS1<sup>myc</sup>, we observed that *pep4* mutant cells, deficient for  
38  
39 429 vacuolar protease activities, displayed higher amounts of the 36 kDa AtUPS1<sup>myc</sup>  
40  
41 430 species than wild type cells even after short induction times, as did *vps23Δ* mutants,  
42  
43 431 impaired in Golgi to vacuole trafficking (data not shown). The increase in plasma  
44  
45 432 membrane amounts of functional forms of tagged AtUPS1 in *rsp5* mutants, attested  
46  
47 433 in exponentially growing cells by increased uracil uptake activity, and on plates by  
48  
49 434 increased 5FU sensitivity might also result from an inhibition of Rsp5p-dependent  
50  
51  
52  
53  
54  
55  
56  
57  
58  
59  
60

1  
2  
3 435 processes at three levels: ERAD, Golgi-to-vacuole trafficking and plasma membrane  
4  
5 436 internalization.  
6

7  
8 437 Rsp5p plays a key role in trafficking of yeast plasma membrane proteins. The  
9  
10 438 present study shows that several viable *rsp5* mutants display increased plasma  
11  
12 439 membrane amounts of a plant transporter, rapidly targeted to the plasma membrane.  
13  
14 440 Strikingly, within the same european network (EFFEXPORT), other laboratories  
15  
16 441 observed, in viable *rsp5* mutants, improved functional expression of several  
17  
18 442 heterologous transporters, including several  $\text{NH}_4^+$  transporters (Rh family) of animal  
19  
20 443 origin (Marini A and André B, personal communication), and increased plasma  
21  
22 444 membrane amounts versus internal fractions of mammalian  $\text{Na}^+/\text{H}^+$  antiporters  
23  
24 445 (Flegegova, H, Haguenaer-Tsapis, R and Sychrova, H. Biochem. Biophys. Acta, in  
25  
26 446 press). In addition, these mutants optimize plasma membrane delivery of tagged  
27  
28 447 versions of the plant AtUPS1, stacked in the ER as a result of folding problems. ER  
29  
30 448 retention is one of the major problems encountered in the case of expression of  
31  
32 449 heterologous plasma membrane proteins in yeast. The increase in steady state  
33  
34 450 plasma membrane amounts of heterologous plant and mammalian transporters,  
35  
36 451 upon expression in viable *rsp5* mutants, show that these cells could be powerful tools  
37  
38 452 to solve the many problems inherent in heterologous expression of membrane  
39  
40 453 proteins, including ER retention.  
41  
42  
43  
44  
45  
46  
47  
48  
49

50 454

## 51 52 455 **Materials and methods**

53  
54 456

### 55 56 457 *Yeast strains and growth conditions*

57  
58 458 Yeast strains were transformed as described by Gietz et al [41]. Cells were grown at  
59  
60 459 30°C in minimal medium (YNB) containing 0.67% yeast nitrogen base without amino

1  
2  
3 460 acids (BD bioscience, NJ, USA), and supplemented with appropriate nutrients. The  
4  
5 461 carbon source was 2% glucose, or 2% galactose plus 0.05% glucose as indicated in  
6  
7  
8 462 the figure legends. Galactose induction was performed on cells grown overnight in  
9  
10 463 2% raffinose plus 0.05% glucose up to an  $A_{600nm}=0.5$ . Galactose (2%) was then  
11  
12 464 added to the medium.

13  
14  
15 465 The disruption of *FUR4* gene was achieved by ORF replacement with long flanking  
16  
17 466 homology regions to the KanMX4 cassette corresponding to the strategy described  
18  
19 467 by Wach [42].  
20  
21

22 468

#### 23 24 469 *Growth tests in the presence of 5-fluorouracil*

25  
26 470 Cells, prototroph for uracil, were cultured overnight in minimal medium containing  
27  
28 471 glucose and spotted on plates containing minimal medium with galactose to induce  
29  
30 472 expression of *FUR4* or *UPS1* variants and supplemented with various concentrations  
31  
32 473 of 5FU (Sigma-Aldrich, Lyon, France). The first drop contained  $3 \cdot 10^4$  cells and each  
33  
34 474 subsequent drop was diluted six-fold compared to the prior drop.  
35  
36  
37  
38  
39

40 475

#### 41 476 *Construction of plasmids*

42  
43 477 DNA manipulations, including restriction analysis and ligations, were performed  
44  
45 478 essentially as described by Maniatis *et al.* [43].  
46  
47

48 479 The control plasmid p195gF-GFP (pRT208) expressing *FUR4*-GFP under the control  
49  
50 480 of the *GAL10* promoter was constructed by cloning a *Pst*I/*Bam*H1 fragment (*FUR4*-  
51  
52 481 GFP) from pFL38gF-GFP [30] into p195gF [28] at the *Pst*I/*Bam*HI site.  
53  
54

55 482 The pGAL-*UPS1* (pRT205) plasmid was constructed by insertion of a *Bam*HI/*Eco*RI  
56  
57 483 fragment encoding *UPS1* (with pFL61-*UPS1* as a template [15]) in the *Bam*HI/*Eco*RI  
58  
59 484 site of pYEF1 [44].  
60

1  
2  
3 485 To construct the plasmid GAL-*UPS1-GFP* (pRT206) we first built the pNBT29  
4  
5 486 plasmid, which contains the yeast enhanced GFP under the control of the GAL10  
6  
7 487 promoter on a multicopy plasmid. For this purpose, a BamHI/NotI fragment encoding  
8  
9 488 GFP was obtained by PCR using the pUG35 plasmid as a template [45] and  
10  
11 489 introduced at the BamHI/NotI site of pYEF1 [44]. Then a BamHI/ClaI fragment  
12  
13 490 encoding AtUPS1 was amplified by PCR using pFL61-*AtUPS1* [15] as a template,  
14  
15 491 and introduced at the BamHI/ClaI site of pNBT29 in frame with the coding sequence  
16  
17 492 of GFP thereby creating a GFP C-terminally tagged version of AtUPS1. To construct  
18  
19 493 the *CYC1-UPS1-GFP* (pRT207) plasmid we cloned the BamHI/EcoRI fragment  
20  
21 494 containing *UPS1-GFP* at the BamHI/EcoRI site of the p416-CYC1 plasmid [46].  
22  
23 495 The pGAL-*UPS1-HA* (pRT204) plasmid was obtained by insertion in the ClaI site of  
24  
25 496 the pYEF2 [44], in frame with the coding sequence of the HA tag, of a fragment  
26  
27 497 encoding *UPS1* obtained by restriction of the plasmid GAL-*UPS1-GFP*.  
28  
29 498 To construct the plasmid pGAL-*UPS1<sup>myc</sup>* (pRT203) two fragments of *UPS1* were  
30  
31 499 amplified separately by PCR using pFL61-*UPS1* as a template. One fragment  
32  
33 500 contained at start an EcoRI and an XbaI site, the 5'- portion of the *UPS1* coding  
34  
35 501 sequence (from ATG to the position 549) and a BamHI site at the end. The other  
36  
37 502 fragment contained a BamHI site at the start, the coding sequence for the c-myc  
38  
39 503 epitope, the 3'- portion of *UPS1* (from position 550 to the stop codon), and an EcoRI  
40  
41 504 and a XhoI site at the end. Both fragments were sequentially cloned in pDR199 [47]  
42  
43 505 using the EcoRI/BamHI sites for the first fragment and BamHI/and XhoI for the  
44  
45 506 second. After sequencing, the complete c-myc tagged *UPS1* sequence was obtained  
46  
47 507 by restriction and subcloned into the Xba I / Xho I sites of the CEN plasmid p416-  
48  
49 508 GAL [46]. Afterwards, the multicopy plasmid pGAL-*UPS1<sup>myc</sup>* was obtained by  
50  
51  
52  
53  
54  
55  
56  
57  
58  
59  
60

1  
2  
3 509 subcloning a SacI/XhoI fragment of the p416-GAL-*UPS1<sup>myc</sup>* into the SacI/XhoI sites  
4  
5 510 of the p426-GAL plasmid [46].  
6  
7

8 511

9  
10 512 *Measurement of uracil uptake.*

11  
12 513 Uracil uptake was measured in exponentially growing cells as previously described.  
13  
14

15 514 Yeast culture (1 ml) was incubated with 5  $\mu$ M [ $^{14}$ C] uracil (ICN biomedical Illkirch,  
16  
17

18 515 France) for 20 sec at 30°C, then quickly filtered through Whatman GF/C filters, which  
19  
20

21 516 were in turn washed twice with ice-cold water and counted for radioactivity. In the  
22  
23

24 517 case of low uracil uptake activity, this basic protocol was slightly modified, with the  
25  
26

27 518 use of two ml samples and incubation for 2 min at 30°C.  
28

29 519

30 520 *Michaelis-Menten kinetics*

31  
32 521 Uracil uptake activities measured at various substrate concentrations were fitted to a  
33  
34

35 522 hyperbola with SIGMA PLOT 5.0, V5 according to Michaelis-Menten kinetics.  
36  
37

38 523

39 524 *Yeast cell extracts, SDS-PAGE and Western immunoblotting*

40  
41 525 Total protein extracts were prepared by the NaOH/Trichloroacetic acid (TCA) lysis  
42  
43

44 526 technique as described in [28]. Proteins were separated by SDS-PAGE on Tricine  
45  
46

47 527 gels and transferred onto nitrocellulose membranes. The membranes were probed  
48  
49

50 528 with monoclonal antibodies against GFP (Roche Diagnostics Meylan, France), or  
51  
52

53 529 myc (9E10 from Roche Diagnostics), or polyclonal antibody against Gas1p (a kind  
54  
55

56 530 gift from H. Riezman). Primary antibodies were detected using horseradish  
57  
58

59 531 peroxidase-conjugated anti-rabbit or anti-mouse IgG secondary antibody (Sigma-  
60  
532

533 532 Aldrich, Lyon, France) revealed by ECL chemiluminescence (Amersham).

533

1  
2  
3 534 *Immunofluorescence*  
4

5 535 Immunofluorescence was performed as described in [48] except that cells were  
6  
7  
8 536 permeabilized with 0.5% Triton X100. The primary antibody was the monoclonal anti-  
9  
10 537 Myc (9E10 from Roche Diagnostics, Meylan, France) and the secondary antibody  
11  
12 538 was an FITC-conjugated goat anti-mouse-IgG (Jackson ImmunoResearch  
13  
14 539 Laboratories, Inc., West Grove, PA). For DNA staining, 1 µg/ml Diamin-Phenylindol-  
15  
16 540 Dihydrochlorid (DAPI) was used. Samples were viewed under an Olympus  
17  
18 541 microscope BY61 using FITC and DAPI filter sets. Image acquisition was performed  
19  
20 542 using a Spot charge-coupled device camera SPOT4.05 .  
21  
22  
23

24 543 For confocal analysis, cells were imaged using an inverted microscope (Leica, Inc.  
25  
26 544 Wetzlar, Germany) and scanning was performed with a True Confocal Scanner LEICA  
27  
28 545 TCS 4D.  
29  
30

31  
32 546

33  
34 547 *Electron microscopy*  
35

36 548 Yeast cells were fixed by adding 200 µl of 50% aqueous glutaraldehyde to 10 ml of  
37  
38 549 growth medium for 10 min and then centrifuged at 5000 g for 10 min at 4°C. After  
39  
40 550 fixation with fresh fixatives for 2 h at 4°C, cells were washed in 0.1 M cacodylate  
41  
42 551 buffer (pH 7.4) and in water. Subsequently, cells were treated with 1% KMnO<sub>4</sub> for 2 h  
43  
44 552 on ice, washed in water and re-suspended in 2% aqueous uranyl acetate for 1 h at  
45  
46 553 4°C. Cells were dehydrated in a graded series of ethanol, infiltrated in a mixture of  
47  
48 554 ethanol and Spurr's resin and embedded in Spurr's low viscosity media. Thin  
49  
50 555 sections were cut, stained with lead citrate and examined in a Tecnai 12 electron  
51  
52  
53 556 microscope (Eindhoven, Netherlands).  
54  
55  
56

57  
58 557  
59  
60

558

TABLE 1. List of strains

Strain	Background	Genotype	Source
MF04	$\Sigma$ 1278b	<i>MATa ura3 trp1 FUR4::KanMX4</i>	This study
MF05	$\Sigma$ 1278b	<i>MATa ura3 trp1 rsp5<math>\Delta</math>C2 FUR4::kanMX4</i>	This study
MF06	$\Sigma$ 1278b	<i>Mata ura3 trp1 npi1 FUR4::kanMX4</i>	This study
27061b	$\Sigma$ 1278b	<i>Mata ura3 trp1</i>	[19]
27064b	$\Sigma$ 1278b	<i>Mata ura3 trp1 npi1</i>	[19]
BY4741	BY	<i>Mata leu2<math>\Delta</math> met15<math>\Delta</math> ura3<math>\Delta</math> his3<math>\Delta</math></i>	Euroscarf

559

560

561

TABLE 2. List of plasmids

Plasmid	Characteristics	Source
pPGK- <i>UPS1</i> (PFL61- <i>UPS1</i> )	2 $\mu$ , <i>URA3</i> prom. <i>PGK-UPS1</i>	[15]
pGAL (PYeF2)	2 $\mu$ , <i>URA3</i> , prom. <i>GAL10</i> , <i>Cter HA</i>	[44]
pGAL- <i>FUR4</i> (pFL38gF)	CEN, <i>URA3</i> , prom. <i>GAL10</i> , <i>FUR4</i>	[30]
p195gF	2 $\mu$ , <i>URA3</i> , prom. <i>GAL10</i> , <i>FUR4</i>	[28]
p195gF-GFP (pRT208)	2 $\mu$ , <i>URA3</i> , prom. <i>GAL10-FUR4-GFP</i>	This study
pGAL- <i>UPS1-HA</i> (pRT204)	2 $\mu$ , <i>URA3</i> , prom. <i>GAL10</i> , <i>UPS1-HA</i>	This study
pGAL- <i>UPS1</i> (pRT205)	2 $\mu$ , <i>URA3</i> , prom. <i>GAL10</i> , <i>UPS1</i>	This study
pGAL- <i>UPS1-GFP</i> (pRT206)	2 $\mu$ , <i>URA3</i> , prom. <i>GAL10</i> , <i>UPS1-GFP</i>	This study
pCYC1- <i>UPS1-GFP</i> (pRT207)	CEN, <i>URA3</i> , prom. <i>CYC1</i> , <i>UPS1-GFP</i>	This study
pGAL- <i>UPS1<sup>myc</sup></i> (pRT203)	2 $\mu$ , <i>URA3</i> , prom. <i>GAL10</i> , <i>UPS1-myc</i>	This study

562

1  
2  
3 563 **Figure 1: Comparison of uracil uptake activity of *Arabidopsis thaliana* UPS1**  
4  
5 564 **expressed in yeast and endogenous uracil permease Fur4p.**

6  
7  
8 565 A: 5-Fluorouracil (5FU) sensitivity. *fur4*Δ cells transformed with either pGAL (empty  
9  
10 566 vector), pGAL-*UPS1* or pGAL-*FUR4* were grown on galactose containing plates  
11  
12 567 supplemented or not with 1μM 5FU (toxic analog of uracil).

13  
14  
15 568 B: Uracil uptake activity of AtUPS1 compared to Fur4p. *fur4*Δ strains transformed  
16  
17 569 with pGAL (white), pGAL-*UPS1*(grey) or pGAL-*FUR4* (black) were grown to  
18  
19 570 exponential phase in galactose containing medium and used for measurement of  
20  
21 571 [<sup>14</sup>C] uracil uptake as described in Materials and Methods. Results are the average of  
22  
23 572 four measures (two measures in two independent experiments).  
24  
25  
26  
27 573

28  
29 574 **Figure 2: Intracellular trafficking of AtUPS1 in yeast.**

30  
31  
32 575 A: *fur4*Δ strains transformed with pGAL-*UPS1* (triangle) or pGAL-*FUR4* (circle) were  
33  
34 576 grown with raffinose as a carbon source. Galactose was then added to induce  
35  
36 577 expression of *AtUPS1* and *FUR4*. The kinetics of plasma membrane delivery of  
37  
38 578 AtUPS1 and Fur4p was determined by quantification of [<sup>14</sup>C] uracil uptake every 30  
39  
40 579 minutes after galactose induction. Results at each time point are the average of two  
41  
42 580 independent measurements.  
43  
44  
45

46 581 B: *fur4*Δ strains transformed with pGAL-*UPS1* (triangle) or pGAL-*FUR4* (circle) were  
47  
48 582 grown in galactose containing medium. Protein synthesis was inhibited by addition of  
49  
50 583 cycloheximide (CHX) (100μg/ml). Uracil uptake activity was measured at various time  
51  
52 584 points (two measurements) after CHX addition. Results are shown as the percentage  
53  
54 585 of initial activities.  
55  
56  
57  
58 586  
59  
60

1  
2  
3 587 **Figure 3: Expression of C-terminally GFP tagged AtUPS1 promotes ER**  
4  
5 588 **proliferation in yeast**  
6

7  
8 589 A: *fur4*Δ cells transformed with pGAL, pGAL-*UPS1-HA*, pGAL-*UPS1-GFP* and  
9  
10 590 *pCYC1-UPS1-GFP* were tested for growth on plates containing or not 5-fluorouracil  
11  
12 591 (0,75 μM).  
13  
14

15 592 B and C: *fur4*Δ cells transformed with pCYC-*UPS1-GFP*, pGAL-*UPS1-GFP* or pGAL-  
16  
17 593 *Fur4-GFP* were grown to mid exponential phase either in glucose, or in raffinose  
18  
19 594 containing medium in the case of strains bearing a plasmid with a GAL promoter.  
20  
21 595 Galactose was then added to induce *AtUPS1-GFP* or *Fur4-GFP* expression. At the  
22  
23 596 indicated times, after galactose addition or after growth in glucose containing media  
24  
25 597 (in the case of pCYC-*UPS1-GFP*), cells were observed by fluorescence microscopy  
26  
27 598 (B) and protein extracts were prepared, resolved by SDS PAGE and analysed by  
28  
29 599 Western immunoblotting using an anti-GFP antibody (C)  
30  
31

32 600 D: *fur4*Δ cells expressing pGAL and pGAL-*UPS1-GFP* grown overnight in galactose  
33  
34 601 containing media were processed for electron microscopy. White arrows indicate the  
35  
36 602 endoplasmic reticulum and N the nucleus.  
37  
38  
39  
40

41 603

42  
43 604 **Figure 4: Intracellular fate of myc tagged version of AtUPS1**  
44

45  
46 605 A: *fur4*Δ cells transformed with pGAL, pGAL-*UPS1*, and pGAL-*UPS1<sup>myc</sup>* were tested  
47  
48 606 for 5-fluorouracil (1 μM) sensitivity on plates.  
49

50  
51 607 B: [<sup>14</sup>C] uracil uptake activity of *fur4*Δ cells transformed with pGAL-*FUR4*, pGAL-  
52  
53 608 *UPS1* and pGAL-*UPS1<sup>myc</sup>* grown to mid exponential phase on galactose containing  
54  
55 609 medium. Results are the average of two independent measures.  
56

57  
58 610 C: *fur4*Δ strains transformed with pGAL-*UPS1* (triangle) or pGAL-*UPS1<sup>myc</sup>* (square)  
59  
60 611 were grown to mid log phase in raffinose containing medium and galactose was then

1  
2  
3 612 added to induce expression of the transporter. The kinetics of plasma membrane  
4  
5 613 delivery of AtUPS1 or Fur4p were determined by quantification of [<sup>14</sup>C] uracil uptake  
6  
7  
8 614 at various times after galactose induction.  
9

10 615 D: *fur4*Δ strains transformed with pGAL-UPS1 (triangle) or pGAL-UPS1<sup>myc</sup> (square)  
11  
12 616 were grown in galactose containing medium. Uracil uptake activity was measured at  
13  
14  
15 617 different time points after inhibition of protein synthesis by addition of CHX  
16  
17 618 (100μg/ml). Results are shown as the percentage of initial activity.  
18

19  
20 619 E: WT cells transformed with pGAL-UPS1<sup>myc</sup> were grown to mid log phase in  
21  
22 620 raffinose containing medium. Galactose was then added to induce transporter  
23  
24 621 expression. Protein extracts were prepared at indicated times and proteins were  
25  
26 622 resolved by SDS PAGE and analysed by Western immunoblotting using an anti-myc  
27  
28 623 antibody to detect the transporter and an anti-Gas1p as a loading control.  
29  
30  
31

32 624

33  
34 625 **Figure 5: Intracellular localization of UPS1<sup>myc</sup> after galactose induction.**

35  
36 626 A: *fur4*Δ cells transformed with pGAL-UPS1<sup>myc</sup> were grown overnight in raffinose  
37  
38 627 containing media. Galactose was added during exponential growth phase. Aliquots  
39  
40 628 were withdrawn at various time points, cells were fixed and processed for  
41  
42 629 immunofluorescence. AtUPS1<sup>myc</sup> was detected using an anti-myc antibody as  
43  
44 630 described in Materials and Methods. The nuclei were stained using DAPI.  
45  
46 631 Fluorescence was observed under an Olympus microscope.  
47  
48  
49

50  
51 632 (Note that, as it is often the case for multicopy plasmid and galactose induction, only  
52  
53 633 a subset of the cells within the population was stained with the anti-myc antibody)

54  
55 634 B: The same preparations as in (A) were also visualized using confocal microscopy.  
56  
57 635 One section is presented for each time point.  
58  
59  
60

60 636

1  
2  
3 637 Figure 6: **Mutations in *RSP5* improve functional expression in yeast of tagged**  
4  
5 638 **and untagged UPS1**

6  
7  
8 639 A: *fur4* $\Delta$ , *rsp5* $\Delta$ *C2 fur4* $\Delta$  and *npi1 fur4* $\Delta$  cells transformed with pPGK-UPS1, pGAL-  
9  
10 640 UPS1, pGAL-UPS1-GFP or pGAL-UPS1<sup>myc</sup> were grown in glucose containing  
11  
12 641 medium and spotted either on glucose (pPGK-UPS1) or on galactose containing  
13  
14 642 plates (pGAL plasmids) with or without 5-fluorouracil as indicated. Different 5FU  
15  
16 643 concentrations were used in order to differentiate optimally the growth of each of the  
17  
18 644 tested strains with regard to the various plasmids: concentration was lower in the  
19  
20 645 case of galactose-induced cells expressing untagged and myc-tagged AtUPS1 that  
21  
22 646 display greater uracil uptake activities than cells expressing GFP-tagged AtUPS1, or  
23  
24 647 untagged AtUPS1 under the control of the PGK promoter. In all cases, growth was  
25  
26 648 tested using a whole range of 5FU concentrations, and a selection of representative  
27  
28 649 plates is shown.

29  
30  
31  
32  
33  
34 650 B: *fur4* $\Delta$  (triangle), *rsp5* $\Delta$ *C2 fur4* $\Delta$  (square) and *npi1 fur4* $\Delta$  (diamond) transformed  
35  
36 651 with pGAL-UPS1-GFP or pGAL-UPS1<sup>myc</sup> were grown to mid log phase in raffinose  
37  
38 652 containing media and the expression of the various transporters was induced by  
39  
40 653 addition of galactose. Plasma membrane delivery of the transporters was assessed  
41  
42 654 by measuring uracil uptake activity at different time points after galactose addition.

43  
44  
45 655 C: Induction of AtUPS1<sup>myc</sup> was monitored in *WT* and *npi1* cells by Western blot  
46  
47 656 analysis of aliquots withdrawn at several time points after addition of galactose.  
48  
49 657 Proteins were resolved by SDS polyacrylamide gel electrophoresis and analyzed by  
50  
51 658 immunoblotting with anti-myc antibodies for quantification of transporter expression  
52  
53 659 and anti-Gas1p as loading control.

54  
55  
56  
57  
58 660

## 661 **Acknowledgements**

662 We thank H. Riezman for the kind gift of antibodies, Antonia Kropfingher for editorial  
663 assistance, and the members of RHT's laboratory for helpful discussions and  
664 comments on the manuscript and. We are grateful to Sophie Le Panse for electron  
665 microscopy. We also thank Jennifer Molinari, Youri Lokossa, Ludovic Warroux and  
666 Yvonne Sauermann for technical help. This work was supported by a grant to M.D.  
667 from the Deutsche Forschungsgemeinschaft (DE 817/1-1).The work done in RHT's  
668 lab was supported by the Centre National de la Recherche Scientifique, the  
669 Universities Paris 6 and Paris 7, by a grant from the Association pour la Recherche  
670 contre le Cancer (ARC) (grant no. 3298), and by an European Union program  
671 (EFFEXPORT, contract QLRT-2001-00533). Marine Froissard, Naïma Belgareh-  
672 Touzé and Jennifer Molinari received fellowships from this program. We are  
673 especially indebted to Bruno Andre, coordinator of the EFFEXPORT program, for his  
674 constant support.

675

## 676 **References**

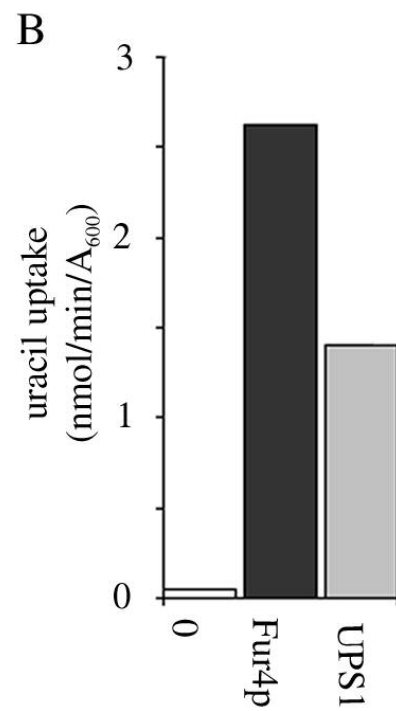
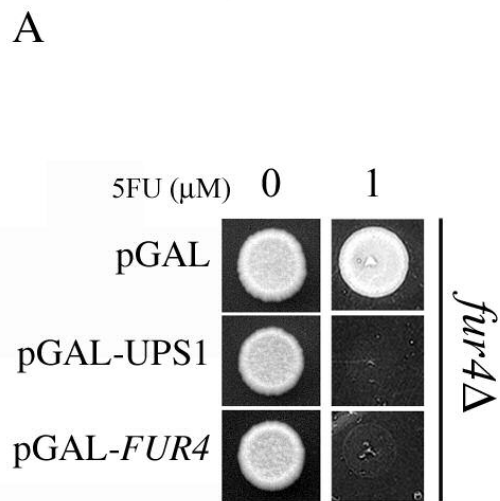
677

- 678 (1) Schwacke, R.; Schneider, A.; van der Graaff, E.; Fischer, K.; Catoni, E; M., D.;  
679 Frommer, W.; Flugge, U.; Kunze, R. *Plant Physiol.* 2003, *131*, 16-26.
- 680 (2) Andre, B. *Yeast* 1995, *11*, 1575-611.
- 681 (3) Nelissen, B.; De Wachter, R.; Goffeau, A. *FEMS Microbiol Rev* 1997, *21*, 113-34.
- 682 (4) Van Belle, D.; Andre, B. *Curr Opin Cell Biol* 2001, *13*, 389-98.
- 683 (5) Winzeler, E. A.; Shoemaker, D. D.; Astromoff, A.; Liang, H.; Anderson, K.; Andre,  
684 B.; Bangham, R.; Benito, R.;et al. *Science* 1999, *285*, 901-6.

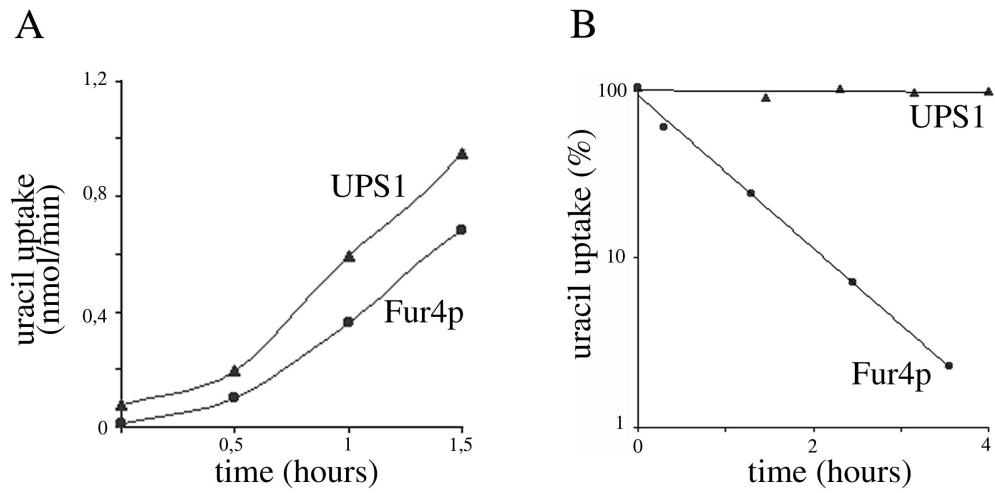
- 1  
2  
3 685 (6) Frommer, W. B.; Ninnemann, O. *Annu. Rev. Plant Physiol. Plant Mol. Biol.* 1995, 46,  
4  
5 686 419-444.  
6  
7  
8 687 (7) Barbier-Brygoo, H.; Gaymard, F.; Rolland, N.; Joyard, J. *Trends Plant Sci* 2001, 6,  
9  
10 688 577-85.  
11  
12 689 (8) Dreyer, I.; Horeau, C.; Lemaillet, G.; Zimmermann, S.; Bush, D. R.; Rodriguez-  
13  
14 690 Navarro, A.; Schachtman, D. P.; Spalding, E. P.; Sentenac, H.; Gaber, R. F. *J. Exp.*  
15  
16 691 *Bot.* 1999, 50, 1073-1087.  
17  
18 692 (9) Bush, D. R. *Curr Opin Plant Biol* 1999, 2, 187-91.  
19  
20 693 (10) Palmgren, M. G.; Christensen, G. *J Biol Chem* 1994, 269, 3027-33.  
21  
22 694 (11) de Kerchove d'Exaerde, A.; Supply, P.; Dufour, J. P.; Bogaerts, P.; Thines, D.;  
23  
24 695 Goffeau, A.; Boutry, M. *J Biol Chem* 1995, 270, 23828-37.  
25  
26 696 (12) Niebauer, R. T.; Wedekind, A.; Robinson, A. S. *Protein Expr Purif* 2004, 37, 134-43.  
27  
28 697 (13) Makuc, J.; Cappellaro, C.; Boles, E. *FEMS Yeast Res* 2004, 4, 795-801.  
29  
30 698 (14) Wiczorke, R.; Dlugai, S.; Krampe, S.; Boles, E. *Cell Physiol Biochem* 2003, 13, 123-  
31  
32 699 34.  
33  
34 700 (15) Desimone, M.; Catoni, E.; Ludewig, U.; Hilpert, M.; Schneider, A.; Kunze, R.;  
35  
36 701 Tegeder, M.; Frommer, W. B.; Schumacher, K. *Plant Cell* 2002, 14, 847-56.  
37  
38 702 (16) Schmidt, A.; Su, Y. H.; Kunze, R.; Warner, S.; Hewitt, M.; Slocum, R. D.; Ludewig,  
39  
40 703 U.; Frommer, W. B.; Desimone, M. *J Biol Chem* 2004, 279, 44817-24.  
41  
42 704 (17) Hagenauer-Tsapis, R.; André, B. In *Control of transmembrane transport*; Boles E  
43  
44 705 and Krämer, R., Ed.; Springer Verlag, 2004.  
45  
46 706 (18) Garnier, C.; Blondel, M. O.; Hagenauer-Tsapis, R. *Mol Microbiol* 1996, 21, 1061-73.  
47  
48 707 (19) Galan, J. M.; Moreau, V.; Andre, B.; Volland, C.; Hagenauer-Tsapis, R. *J Biol Chem*  
49  
50 708 1996, 271, 10946-52.  
51  
52 709 (20) Rotin, D.; Staub, O.; Hagenauer-Tsapis, R. *J Membr Biol* 2000, 176, 1-17.  
53  
54  
55  
56  
57  
58  
59  
60

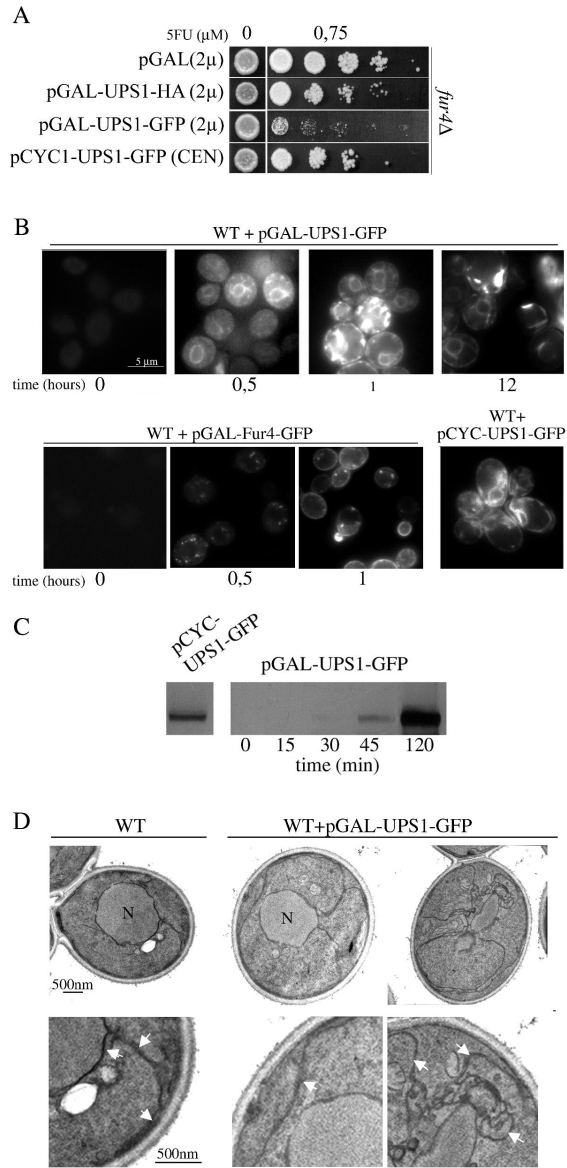
- 1  
2  
3 710 (21) Blondel, M. O.; Morvan, J.; Dupre, S.; Urban-Grimal, D.; Haguenaer-Tsapis, R.;  
4  
5 711 Volland, C. *Mol Biol Cell* 2004, 15, 883-95.  
6  
7  
8 712 (22) Pizzirusso, M.; Chang, A. *Mol Biol Cell* 2004, 15, 2401-9.  
9  
10 713 (23) Hoppe, T.; Matuschewski, K.; Rape, M.; Schlenker, S.; Ulrich, H. D.; Jentsch, S. *Cell*  
11  
12 714 2000, 102, 577-86.  
13  
14  
15 715 (24) Rodriguez, M. S.; Gwizdek, C.; Haguenaer-Tsapis, R.; Dargemont, C. *Traffic* 2003,  
16  
17 716 4, 566-75.  
18  
19  
20 717 (25) Hein, C.; Springael, J. Y.; Volland, C.; Haguenaer-Tsapis, R.; Andre, B. *Mol*  
21  
22 718 *Microbiol* 1995, 18, 77-87.  
23  
24  
25 719 (26) Wang, G.; McCaffery, J. M.; Wendland, B.; Dupre, S.; Haguenaer-Tsapis, R.;  
26  
27 720 Huibregtse, J. M. *Mol Cell Biol* 2001, 21, 3564-75.  
28  
29  
30 721 (27) Moreau, V.; Galan, J. M.; Devilliers, G.; Haguenaer-Tsapis, R.; Winsor, B. *Mol Biol*  
31  
32 722 *Cell* 1997, 8, 1361-75.  
33  
34  
35 723 (28) Volland, C.; Urban-Grimal, D.; Geraud, G.; Haguenaer-Tsapis, R. *J Biol Chem* 1994,  
36  
37 724 269, 9833-41.  
38  
39  
40 725 (29) Dupre, S.; Haguenaer-Tsapis, R. *Mol Cell Biol* 2001, 21, 4482-94.  
41  
42  
43 726 (30) Marchal, C.; Dupre, S.; Urban-Grimal, D. *J Cell Sci* 2002, 115, 217-26.  
44  
45  
46 727 (31) Bugnicourt, A.; Froissard, M.; Sereti, K.; Ulrich, H. D.; Haguenaer-Tsapis, R.;  
47  
48 728 Galan, J. M. *Mol Biol Cell* 2004, 15, 4203-14.  
49  
50  
51 729 (32) Dupre, S.; Urban-Grimal, D.; Haguenaer-Tsapis, R. *Biochim Biophys Acta* 2004,  
52  
53 730 1695, 89-111.  
54  
55  
56 731 (33) Bachmair, A.; Novatchkova, M.; Potuschak, T.; Eisenhaber, F. *Trends Plant Sci* 2001,  
57  
58 732 6, 463-70.  
59  
60 733 (34) Morvan, J.; Froissard, M.; Haguenaer-Tsapis, R.; Urban-Grimal, D. *Traffic* 2004, 5,  
734 383-92.

- 1  
2  
3 735 (35) Springael, J. Y.; De Craene, J. O.; Andre, B. *Biochem Biophys Res Commun* 1999,  
4  
5 736 257, 561-6.  
6  
7  
8 737 (36) Dunn, R.; Hicke, L. *J Biol Chem* 2001, 276, 25974-81.  
9  
10 738 (37) Katzmann, D. J.; Sarkar, S.; Chu, T.; Audhya, A.; Emr, S. D. *Mol Biol Cell* 2004, 15,  
11  
12 739 468-80.  
13  
14  
15 740 (38) Dunn, R.; Klos, D. A.; Adler, A. S.; Hicke, L. *J Cell Biol* 2004, 165, 135-44.  
16  
17 741 (39) Haynes, C. M.; Caldwell, S.; Cooper, A. A. *J Cell Biol* 2002, 158, 91-101.  
18  
19 742  
20  
21  
22 743 (40) Soetens, O.; De Craene, J. O.; Andre, B. *J Biol Chem* 2001, 276, 43949-57.  
23  
24 744 (41) Gietz, D.; St Jean, A.; Woods, R. A.; Schiestl, R. H. *Nucleic Acids Res* 1992, 20,  
25  
26 745 1425.  
27  
28  
29 746 (42) Wach, A. *Yeast* 1996, 12, 259-65.  
30  
31 747 (43) Maniatis, T.; Fritsch, E. F.; Sambrook, J. *Molecular Cloning: A Laboratory Manual*;  
32  
33 Cold Spring Harbor Laboratory: Cold Spring Harbor, N.Y., 1982.  
34 748  
35  
36 749 (44) Cullin, C.; Minvielle-Sebastia, L. *Yeast* 1994, 10, 105-12.  
37  
38 750 (45) Niedenthal, R. K.; Riles, L.; Johnston, M.; Hegemann, J. H. *Yeast* 1996, 12, 773-86.  
39  
40 751 (46) Mumberg, D.; Muller, R.; Funk, M. *Gene* 1995, 156, 119-22.  
41  
42 752 (47) Rentsch, D.; Laloi, M.; Rouhara, I.; Schmelzer, E.; Delrot, S.; Frommer, W. B. *FEBS*  
43  
44 753 *Lett* 1995, 370, 264-8.  
45  
46  
47  
48 754 (48) Belgareh-Touze, N.; Avaro, S.; Rouille, Y.; Hoflack, B.; Haguenaer-Tsapis, R. *Mol*  
49  
50 755 *Biol Cell* 2002, 13, 1694-708.  
51  
52  
53 756  
54  
55 757  
56  
57  
58  
59  
60



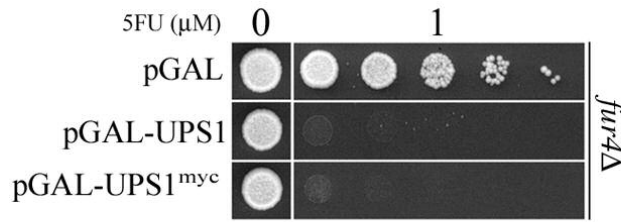
Review



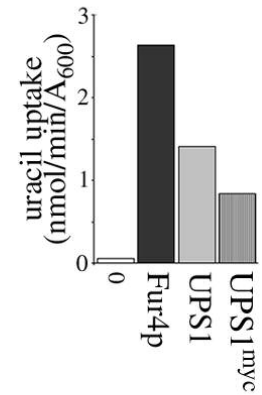


1  
2  
3  
4  
5  
6  
7  
8  
9  
10  
11  
12  
13  
14  
15  
16  
17  
18  
19  
20  
21  
22  
23  
24  
25  
26  
27  
28  
29  
30  
31  
32  
33  
34  
35  
36  
37  
38  
39  
40  
41  
42  
43  
44  
45  
46  
47  
48  
49  
50  
51  
52  
53  
54  
55  
56  
57  
58  
59  
60

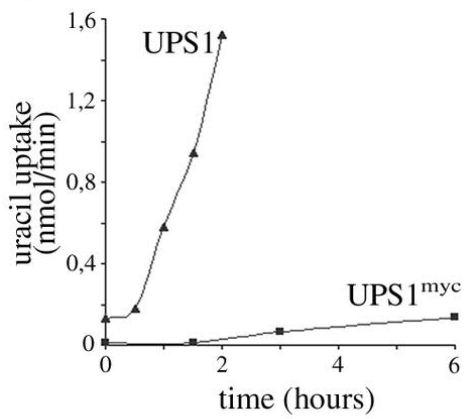
A



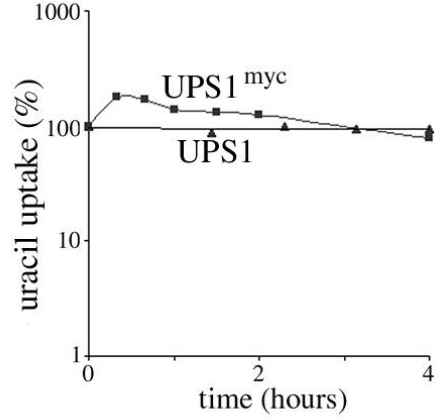
B



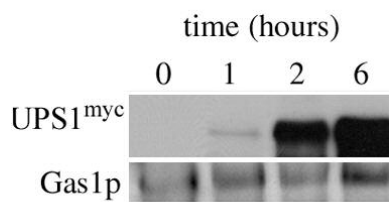
C

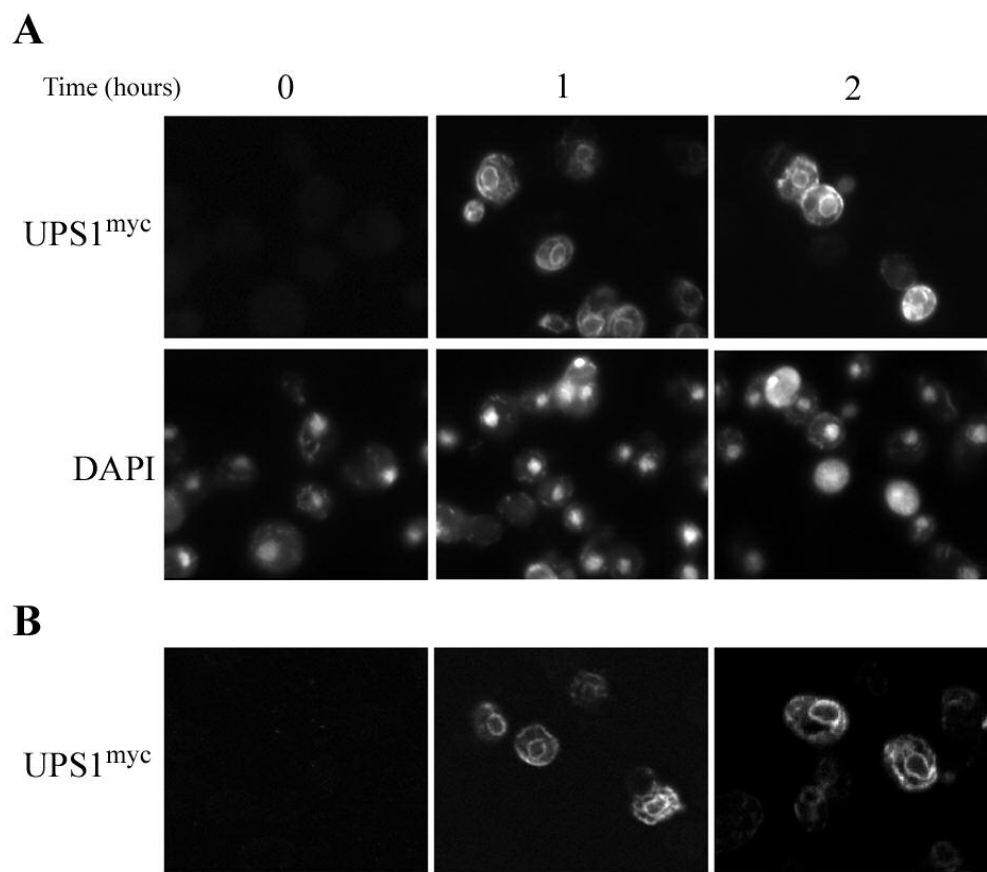


D

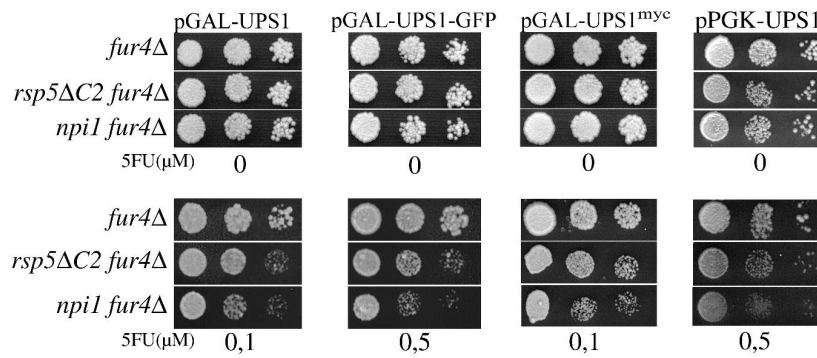


E

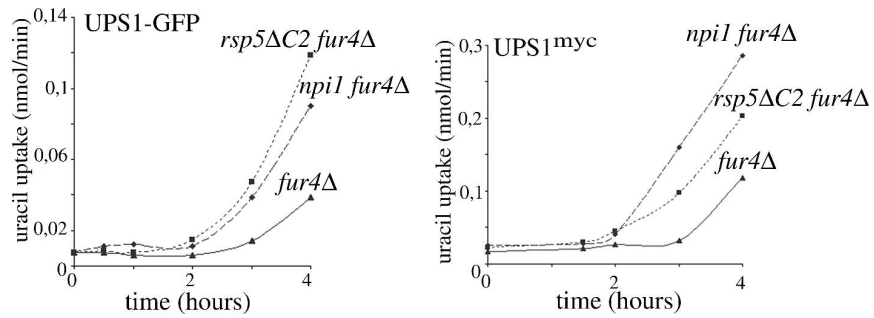




A



B



C

